JOURNAL OF COMPUTATIONAL PHYSICS 108, 209–217 (1993)

Upwind Finite Difference Solution of Boltzmann Equation Applied to Electron Transport in Semiconductor Devices

EMAD FATEMI*

Institute for Mathematics and Its Applications, Minneapolis, Minnesota 55455

AND

FAROUKH ODEH†

IBM T. J. Watson Research Center, Yorktown Heights, New York 10598

Received June 1, 1992; revised November 30, 1992

We present a new numerical method for solving the Boltzmann–Poisson system which describes charge transport in semiconductor devices. The Boltzmann equation is reduced from three dimensions in velocity space to two by taking the electric field parallel to the z axis, which implies invariance of the probability density function under rotation around the z axis. We develop a finite difference discretization of the Boltzmann equation in one spatial dimension and two-dimensional velocity space, coupled to the Poisson equation. The system of equations obtained by taking the first five moments of the Boltzmann equation coupled to the Poisson equation is known as the hydrodynamic model in semiconductor modeling. A comparison of the numerical results from our method and the hydrodynamic model is given. Also a numerical investigation is done with respect to the heat conduction, viscosity, and momentum relaxation terms in the hydrodynamic model.

1. INTRODUCTION

Charge transport in semiconductor devices is modeled semi-classically via a system consisting of the Boltzmann transport equation, BTE, coupled to the Poisson equation. The Boltzmann equation is an integro-differential equation in seven dimensions, with three dimensions in space, three in velocity space, and one in time. Full discretization of the BTE in seven dimensions is out of the range of existing computers. A variety of numerical methods have been designed to solve the Boltzmann equation. A very popular method for solving the BTE is the Monte Carlo method. For a comprehensive and tutorial review of this method, with emphasis on charge transport in semiconductor devices, we refer the reader to the article by Jacoboni and Reggiani [10]. The Monte Carlo method relies on random sampling and the results are often noisy. Accurate coupling of the two equations in Monte Carlo calculations is a non-trivial task. Another approach to solving BTE is the particle method. In this approach, the collision integrals are calculated deterministically [13].

We develop an upwind finite difference approximation for the Boltzmann–Poisson system. Forward Euler time differencing is used to discretize the Boltzmann equation in time. A general upwind scheme is designed to handle the differential terms in the Boltzmann equation. The discretization is designed such that mass is conserved in each time step. The collision integrals are approximated by simple trapezoidal rule. The result of the approximation is a matrix that is calculated once in the beginning of the calculation. This method is closely related to the methods developed for solving the kinetic equation for neutron transport [11] and to the methods developed by Chorin [3] and Sod [16] for solving the Boltzmann equation for a steady shock wave.

The first five moments of the Boltzmann equation taken in the velocity space are conservation laws for mass, momentum, and energy. The conservation law system consists of five equations with 14 dependent variables in three-dimensional space. The system is usually closed with constitutive relations which are derived from certain assumptions about the shape of the probability density function in the velocity space. The hydrodynamic model in semiconductor modeling is derived with the assumption of pressure tensor to be scalar and heat flux to be defined by the Fourier law [1, 4]. The hydrodynamic model consists of

* This research was supported in part by the Institute for Mathematics and its Applications with funds provided by the National Science Foundations.

† Regrettably Faroukh is no longer with us. His sudden death was a big loss for his fiends and colleagues. He will be remembered for his gentle and generous soul.

0021-9991/93 $5.00

the Euler equations of gas dynamics with source terms and the heat conduction term coupled to the Poisson equation. In the hydrodynamic model scattering terms are replaced with relaxation time approximations.

A simpler and older model that is widely used for industrial applications is *drift–diffusion*. The drift–diffusion system is conservation of the mass equation and a simplified version of conservation of the momentum equation. The simplified momentum equation is derived by assuming temperature to be constant and the Mach number of the flow to be small. The drift–diffusion model loses its accuracy as the size of the device becomes less than one micron. The numerical results from the hydrodynamic model confirm that it is more accurate than the drift–diffusion model in the submicron regime.

We develop an upwind finite differencing method to solve the Boltzmann–Poisson equation numerically. Once the distribution function is calculated, we evaluate the moments of the distribution function numerically and recover various terms in the hydrodynamic model. This procedure enables us to test various hypotheses and approximations for the constitutive laws in the hydrodynamic model. The hydrodynamic model is solved using a sixth-order essentially non-oscillatory, ENO, shock capturing algorithm [4, 15]. The ENO methods were designed originally for computation of gas flows with shocks and flows in high Mach number regimes. The ENO method is based on interpolating a sixth-order polynomial to the data in an adaptive fashion. The stencil points are chosen such that data from the smooth part of the solution is used for the interpolation. The high order method is proven to be effective in resolving the solution in high gradient regions.

2. BOLTZMANN–POISSON SYSTEM

We represent by $f(\mathbf{x}, \mathbf{u}, t)$ the probability density function of electrons, where $\mathbf{x} = (x, y, z)$ is the space variable, $\mathbf{u} = (u, v, w)$ is the velocity variable, and t is the time variable. The dynamics of electrons is modeled by

$$f_t + \mathbf{u}\cdot\nabla_{\mathbf{x}} f + \frac{e}{m}\nabla\phi\cdot\nabla_{\mathbf{u}} f = \int s(\mathbf{u}', \mathbf{u}) f(\mathbf{u}')\, d\mathbf{u}' - \int s(\mathbf{u}, \mathbf{u}') f(\mathbf{u})\, d\mathbf{u}', \tag{1}$$

$$\nabla\cdot(\varepsilon\nabla\phi) = e(-N_D(\mathbf{x}) + \int f(\mathbf{u})\, d\mathbf{u}), \tag{2}$$

$$(F_x, F_y, F_z) = \mathbf{F} = \frac{-e}{m}\mathbf{E} = \frac{e}{m}\nabla\phi, \qquad n = \int f(\mathbf{u})\, d\mathbf{u};$$

$s(\mathbf{u}, \mathbf{u}')$ is the scattering operator, ϕ is the electric potential, $\mathbf{E}$ is the electric field, $N_D(\mathbf{x})$ is the density of donors, e is the charge of an electron, ε is the permittivity in the crystal, and $n = \int f(\mathbf{u})\, d\mathbf{u}$ is the density of electrons. We consider only the scattering of electrons from lattice sites in the scattering operator and the electron–electron interaction is neglected. The electron–electron scattering can be easily incorporated in our numerical method. Note that $N_D(\mathbf{x})$ in general is a discontinuous function and jumps of several orders of magnitude in N_D are normal in a device.

We scale the equations in the following fashion:

$$\bar{t}\tau_t = t, \qquad \bar{\mathbf{x}}L = \mathbf{x}, \qquad \bar{\mathbf{u}}U = \mathbf{u},$$

$$\frac{\bar{S}}{\tau_p} = S, \qquad \bar{\phi}\left(\frac{mEL}{e}\right) = \phi, \qquad \bar{n}N = n;$$

τ_p is the momentum relaxation time, τ_t is a typical time scale for relaxation of the transients in the time dependent solutions, U is of the order of the saturation velocity of the electrons, E is the maximum electric field in a device, and N is the maximum value of $N_D(x)$. In a typical device there is always an internal electric field around the junctions and E could be high even if the applied voltage is zero. We suppress the bar notation for the scaled quantities and obtain

$$f_t + \left(\frac{U\tau_t}{L}\right)\mathbf{u}\cdot\nabla_{\mathbf{x}} f + \left(\frac{E\tau_t}{U}\right)\nabla\phi\cdot\nabla_{\mathbf{u}} f = \left(\frac{\tau_t}{\tau_p}\right)\left(\int s(\mathbf{u}', \mathbf{u}) f(\mathbf{u}')\, d\mathbf{u}' - \int s(\mathbf{u}, \mathbf{u}') f(\mathbf{u})\, d\mathbf{u}'\right), \tag{3}$$

$$\nabla\cdot(\nabla\phi) = \left(\frac{e^2 LN}{\varepsilon mE}\right)(-N_D + n). \tag{4}$$

There are four non-dimensional parameters in the above system:

$$\frac{U\tau_t}{L}, \qquad \frac{E\tau_t}{U}, \qquad \frac{\tau_t}{\tau_p}, \qquad \frac{e^2 LN}{\varepsilon mE}.$$

We let $\tau_t = L/U$ and then we have

$$\frac{U\tau_t}{L} = 1, \qquad \frac{E\tau_t}{U} \approx 0.675, \qquad \frac{\tau_t}{\tau_p} \approx 5 \sim 50, \qquad \frac{e^2 LN}{\varepsilon mE} \approx 150.$$

We identify the ratio $Kn = \tau_p/\tau_t = \tau_p U/L$ as the Knudsen number of the flow. Note that the quantity $e^2 LN/\varepsilon mE$ represents the stiffness of the system due to the Poisson equation. The stiffness of the problem increases with increasing N and decreases with decreasing L.

From the Boltzmann equation one can obtain conservation laws for the mass, momentum, and energy of the flow.

The average of the quantity $\psi(\mathbf{u})$ in the velocity space is defined by

$$\langle \psi(\mathbf{u}), f \rangle = \int_{-\infty}^{+\infty} \int_{-\infty}^{+\infty} \int_{-\infty}^{+\infty} \psi(\mathbf{u}) f(\mathbf{u})\, d\mathbf{u}.$$

The equation for the evolution of the averaged quantity, $\langle \psi, f \rangle$, is obtained from the Boltzmann equation,

$$\langle \psi, f \rangle_t + \nabla_{\mathbf{x}} \langle \mathbf{u}\psi, f \rangle = \mathbf{F} \langle \nabla_{\mathbf{u}} \psi, f \rangle + \langle \psi, S \rangle. \quad (5)$$

By taking $\psi = m$, $m\mathbf{u}$, and $\frac{1}{2}m\mathbf{u}^2$ one recovers the Euler equations of gas dynamics. These equations for electron transport have been proposed by Bløtekjær [2] and have been studied numerically by [8, 14, 7, 4, 5]. The viscosity solutions of this system have been studied by [6]. In the numerical calculations done in [4], non-physical velocity spikes were observed as electrons cross the channel to the drain. We investigate the source of this inaccuracy by checking the accuracy of the approximations for heat conduction, viscosity, and momentum relaxation terms.

We use the classical closure relations for the compressible gas flow to close the hydrodynamic model [9]. The Chapman–Enskog expansion is obtained by expanding the distribution function for a dilute gas in the parameter $\varepsilon = \lambda/L$, where λ is the mean free path and L is a typical length scale. The zeroth-order term is a displaced Maxwellian for the distribution of the gas. The conservation laws obtained from the zeroth-order approximation is the Euler equations for compressible gas flows. The conservation laws from the first-order approximation is simply the Navier–Stokes system for compressible gas flows.

We repeat here the first-order approximations of the constitutive relations for reference. We define $\mathbf{v}$ to be the average velocity, $\mathbf{v} = \langle \mathbf{u}, f \rangle / \langle 1, f \rangle$. The third moment of the probability density funcion is identified as the heat conduction and is approximated by the Fourier law,

$$\tfrac{1}{2}m \langle |\mathbf{u} - \mathbf{v}|^2 (\mathbf{u} - \mathbf{v}), f \rangle \approx \kappa n \nabla T.$$

The pessure tensor is approximated by a scalar pressure plus the viscous correction,

$$\tfrac{1}{2}m \langle (\mathbf{u} - \mathbf{v})' (\mathbf{u} - \mathbf{v}), f \rangle = \begin{pmatrix} nT_{11} & nT_{12} & nT_{13} \\ nT_{21} & nT_{22} & nT_{23} \\ nT_{31} & nT_{32} & nT_{33} \end{pmatrix} \approx \begin{pmatrix} nT & 0 & 0 \\ 0 & nT & 0 \\ 0 & 0 & nT \end{pmatrix} - \nu \begin{pmatrix} \frac{4}{3}u_x - \frac{2}{3}v_y - \frac{2}{3}w_z & u_y + v_x & w_x + u_z \\ u_y + v_x & \frac{4}{3}v_y - \frac{2}{3}u_x - \frac{2}{3}w_z & w_y + v_z \\ u_z + w_x & v_z + w_y & \frac{4}{3}w_z - \frac{2}{3}u_x - \frac{2}{3}v_y \end{pmatrix},$$

where temperature is defined as $T = (T_{11} + T_{22} + T_{33})/3$. For the coefficient of viscosity we use $\nu = \tau_p nT$ which is based on assuming the momentum relaxation time, τ_p, to be the mean free time. This assumption has not been investigated. The momentum relaxation time is defined by

$$\langle \mathbf{u}S, f \rangle \approx -\langle \mathbf{u}, f \rangle / \tau_p.$$

We use the calculated probability density function from the Boltzmann equation to verify the models for κ and τ_p, as proposed by Baccarani and Wordeman [1]. These models are $\kappa = 3\mu_0 k_b^2 T_0/2e$ and $\tau_p = m\mu_0 T/eT$.

3. TRANSFORMATION TO SPHERICAL COORDINATES

We consider a one-dimensional device where the electric field is in the z axis direction. The probability density function is invariant under rotation around the z axis. Exploiting this property, we do a coordinate transformation in the velocity space from the Cartesian coordinate system to a spherical coordinate system. This enables us to reduce the number of independent variables in the velocity space from three to two. Consider the Boltzmann equation for $f(x, y, z, u, v, w, t)$,

$$f_t + \mathbf{u} \nabla_{\mathbf{x}} f + \mathbf{F} \nabla_{\mathbf{u}} f = \int s(\mathbf{u}', \mathbf{u}) f(\mathbf{u}')\, d\mathbf{u}' - \int s(\mathbf{u}, \mathbf{u}') f(\mathbf{u})\, d\mathbf{u}'.$$

We use the spherical transformation from (k, θ, ϕ) to (u, v, w) via $u = k \sin\theta \cos\phi$, $v = k \sin\theta \sin\phi$, and $w = k \cos\theta$; k is the length of the vector (u, v, w), θ is the angle between the velocity vector and the z axis, and ϕ is the angle around the z axis. The Boltzmann equation in the transformed space is

$$\begin{aligned} f_t &+ k \sin\theta \cos\phi f_x + k \sin\theta \sin\phi f_y + k \cos\phi f_z \\ &+ \{F_x \sin\theta \cos\phi + F_y \sin\theta \sin\phi + F_z \cos\theta\} f_k \\ &+ \left\{ F_x \frac{\cos\phi \cos\theta}{k} + F_y \frac{\sin\phi \cos\theta}{k} - F_z \frac{\sin\theta}{k} \right\} f_\theta \\ &+ \left\{ -F_x \frac{\sin\phi}{k \sin\theta} + F_y \frac{\cos\phi}{k \sin\theta} \right\} f_\phi \\ &= \int s(k', \theta', \phi', k, \theta, \phi) f(k', \theta', \phi')\, k'^2 \sin\theta'\, dk'\, d\theta'\, d\phi' \\ &- \int s(k, \theta, \phi, k', \theta', \phi') f(k, \theta, \phi) \\ &\times k'^2 \sin\theta'\, dk'\, d\theta'\, d\phi'. \end{aligned}$$

f is dependent only on z, k, θ, and t because of the axial symmetry. We introduce a new variable $\mu = \cos\theta$ and then the right-hand side of the Boltzmann equation is

$$f_t + k\mu f_z + F_z \left\{ \mu f_k + \frac{1 - \mu^2}{k} f_\mu \right\}.$$

For discretization purposes we prefer to write it as

$$f_t + k\mu f_z + F_z\left\{\mu f_k + \frac{2\mu f}{k} + \frac{((1-\mu^2)f)_\mu}{k}\right\}.$$

The above definition is motivated by the observation that the combination $\mu f_k + 2\mu f/k$ is not in conservative form, but $k^2(\mu f_k + 2\mu f/k) = \mu(k^2 f)_k$ is in conservative form. The complete transformed system is

$$f_t + k\mu f_z + F_z\left\{\mu f_k + \frac{2\mu f}{k} + \frac{((1-\mu^2)f)_\mu}{k}\right\} \tag{6}$$

$$= 2\pi \int s(k', \mu', k, \mu) f(k', \mu')\, k'^2\, dk'\, d\mu'$$

$$- 2\pi \int s(k, \mu, k', \mu') f(k, \mu)\, k'^2\, dk'\, d\mu',$$

$$\phi_{zz} = \frac{e}{\varepsilon}(n - N_D), \tag{7}$$

$$n = 2\pi \iint f(k, \mu)\, k^2\, dk\, d\mu, \qquad F_z = \frac{e}{m}\phi_z.$$

The above system is completed with the initial value and boundary conditions. For the Poisson equation, we specify the potential at the boundaries of the device, $\phi(0) = 0$ and $\phi(z_{\max}) = 1.0$. For the initial value of f, we specify a Maxwellian distribution with zero mean velocity and temperature of the lattice, T_0:

$$f(z, k, \mu, 0) = \left(\frac{m}{2\pi k_B T_0}\right)^{3/2} \exp\left(-\frac{mk^2}{2k_B T_0}\right).$$

In the Cartesian coordinates, the computational domain is the cross product of the interval $[0, z_{\max}]$ with a shell, inner radius $k_{\min}$, and outer radius $k_{\max}$. In spherical coordinates this domain is transformed into the box: $[0, z_{\max}] \times [k_{\min}, k_{\max}] \times [-1, 1]$. The boundary conditions are determined based on the direction of the characteristic lines (see Fig. 1). There is no need for boundary conditions at $f(z, k, 1)$ and $f(z, k, -1)$ since the characteristics are parallel to the boundary. Also no boundary conditions are necessary for $f(0, k, \mu)$ for $\mu < 0$ and $f(z_{\max}, k, \mu)$ for $\mu > 0$. In the k direction we use zero flux condition for $k_{\max}$:

$$f(z, k_{\max}, \mu) = 0.$$

The boundary condition at the boundary of the removed sphere around the singular point, $k = 0$, is based on identifying the upper part of the hemi-sphere with the lower part. This boundary condition in the transformed domain is

$$f(z, k_{\min}, \mu) = f(z, k_{\min}, -\mu).$$

We study the characteristic lines in (k, μ) space to motivate the above condition. The characteristic lines are defined as integral curves of

$$\frac{dk}{ds} = F_z\mu, \qquad \frac{d\mu}{ds} = \frac{F_z(1-\mu^2)}{k}.$$

In the Cartesian space, (u, v, w), they correspond to

$$\frac{du}{ds} = 0, \qquad \frac{dv}{ds} = 0, \qquad \frac{dw}{ds} = F_z.$$

In the Cartesian space, points (u, v, w) are connected to the points $(u, v, -w)$ through the characteristic lines (see Fig. 2). After removal of the ball, we identify (u, v, w) points with $(u, v, -w)$ points. This is equivalent to identifying

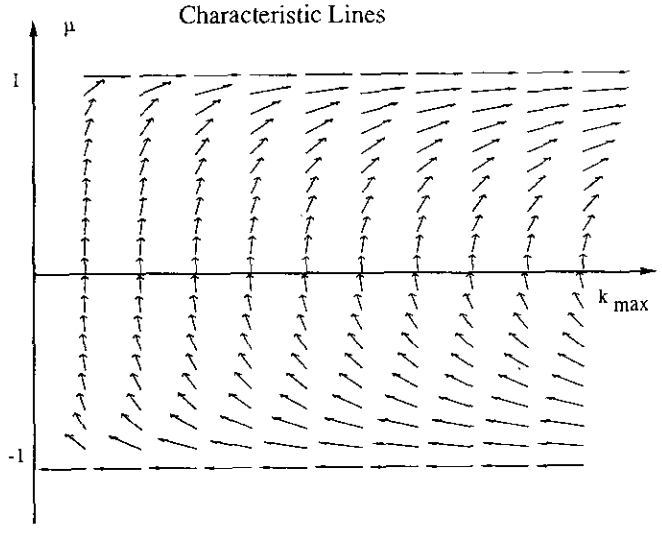

FIG. 1. Characteristic curves in velocity space.

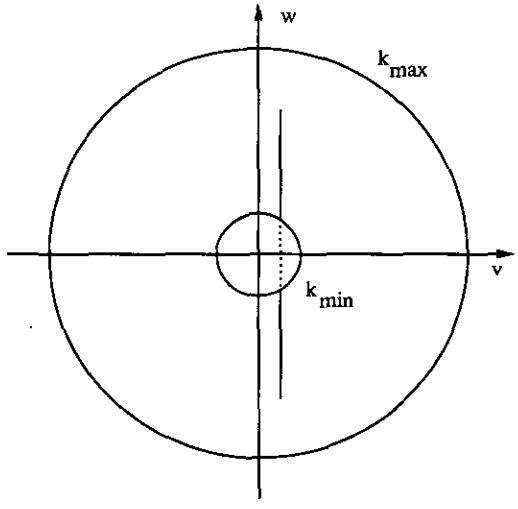

FIG. 2. Boundary conditions for $k_{\min}$.

(k, μ) with $(k, -\mu)$. Finally, we specify the boundary conditions for the inflow and outflow of electrons:

$$f(0, k, \mu) \quad \text{if} \quad \mu > 0, \qquad f(z_{\max}, k, \mu) \quad \text{if} \quad \mu < 0.$$

Choosing the appropriate boundary conditions is part of the physical modeling of the device under consideration; for the ballistic diode we choose $\partial f/\partial z = 0$.

We consider the scattering terms for our calculations [10],

$$\int s(\mathbf{u}', \mathbf{u}) f(\mathbf{u}')\, d\mathbf{u}' - \int s(\mathbf{u}, \mathbf{u}') f(\mathbf{u})\, d\mathbf{u}',$$

where

$$s(\mathbf{u}, \mathbf{u}') = s_{ac}(\mathbf{u}, \mathbf{u}') + s_{op}^{em}(\mathbf{u}, \mathbf{u}') + s_{op}^{abs}(\mathbf{u}, \mathbf{u}'),$$

$$s_{ac}(\mathbf{u}, \mathbf{u}') = \frac{1}{(2\pi)^3}\left(\frac{m}{\hbar}\right)^3 \frac{2\pi k_B T_0 E_{ac}^2}{\hbar u_l^2 \rho}\, \delta[E(\mathbf{u}') - E(\mathbf{u})],$$

$$s_{op}^{em}(\mathbf{u}, \mathbf{u}') = \frac{1}{(2\pi)^3}\left(\frac{m}{\hbar}\right)^3 \frac{\pi (D_t K)^2}{\rho \omega_{op}} \times N_{op}^{+} \delta[E(\mathbf{u}') - E(\mathbf{u}) + \hbar\omega_{op}],$$

$$s_{op}^{abs}(\mathbf{u}, \mathbf{u}') = \frac{1}{(2\pi)^3}\left(\frac{m}{\hbar}\right)^3 \frac{\pi (D_t K)^2}{\rho \omega_{op}} \times N_{op} \delta[E(\mathbf{u}') - E(\mathbf{u}) - \hbar\omega_{op}];$$

E is the energy of an electron and is given by $E(\mathbf{u}) = \frac{1}{2} m \mathbf{u}^2 = \frac{1}{2} m k^2$; m is the reduced mass of an electron, and δ is the delta function.

The corresponding terms in the hydrodynamic model are calculated by computing the integral in spherical coordinates:

$$\langle h, f \rangle = \int_0^{\infty} k^2\, dk \int_{-1}^{1} f(k, \mu)\, d\mu \int_0^{2\pi} h(k, \mu, \phi)\, d\phi.$$

We present a list of the quantities of interest:

$$h(k, \mu, \phi) = 1, u, v, w, u^2, v^2, w^2, uv, vw, wu, uk^2, vk^2, wk^2,$$

$$\langle 1, f \rangle = 2\pi \int_0^{+\infty} \int_{-1}^{1} k^2 f(k, \mu)\, dk\, d\mu,$$

$$\langle w, f \rangle = 2\pi \int_0^{+\infty} \int_{-1}^{1} \mu k^3 f(k, \mu)\, dk\, d\mu,$$

$$\langle v, f \rangle = 0,$$

$$\langle u, f \rangle = 0,$$

$$\langle u^2, f \rangle = \langle v^2, f \rangle = \pi \int_0^{+\infty} \int_{-1}^{1} (1 - \mu^2)\, k^4 f(k, \mu)\, dk\, d\mu,$$

$$\langle w^2, f \rangle = 2\pi \int_0^{+\infty} \int_{-1}^{1} \mu^2 k^4 f(k, \mu)\, dk\, d\mu,$$

$$\langle uv, f \rangle = 0,$$

$$\langle uw, f \rangle = 0,$$

$$\langle vw, f \rangle = 0,$$

$$\langle uk^2, f \rangle = 0,$$

$$\langle vk^2, f \rangle = 0,$$

$$\langle wk^2, f \rangle = 2\pi \int_0^{+\infty} \int_{-1}^{1} \mu k^5 f(k, \mu)\, dk\, d\mu.$$

The heat conduction term is

$$\frac{1}{2} m \left(\langle wk^2, f \rangle - \frac{\langle w, f \rangle}{\langle 1, f \rangle} \{3\langle w^2, f \rangle + \langle u^2, f \rangle + \langle v^2, f \rangle\} + 2 \frac{\langle w, f \rangle^3}{\langle 1, f \rangle^2} \right).$$

Temperature is calculated via

$$T_{11} = \frac{1}{2m} \frac{\langle u^2, f \rangle - \langle u, f \rangle^2}{\langle 1, f \rangle},$$

$$T_{33} = \frac{1}{2m} \frac{\langle w^2, f \rangle - \langle w, f \rangle^2}{\langle 1, f \rangle}.$$

4. THE BALLISTIC DIODE PROBLEM

As a model problem, we simulate the flow of electrons in a submicron $n^+ - n - n^+$ silicon diode. This device models the channel in a MOSFET. The diode begins with a n^+ "source" region, is then followed by a n "channel" region, and ends with a n^+ "drain" region. The effects of holes may be neglected for the ballistic diode problem. For a discussion of the units and the proper constants, we refer the reader to Fatemi, Jerome, and Osher [4]. For the constants that are not in the above reference, we use the following values:

$$N_{op} = (e^{\hbar\omega_{op}/k_B T_0} - 1)^{-1}, \qquad N_{op}^{+} = N_{op} + 1$$

$$E_{ac} = 5.0 \text{ eV}, \qquad \hbar = 1.055 \times 10^{-34}, \qquad u_l = 9.0 \times 10^5 \text{ cm/s}$$

$$\rho = 2.33 \text{ g/cm}^3, \qquad D_t K = 15.5 \times 10^8 \text{ eV/cm},$$

$$\hbar\omega = 0.063 \text{ eV}.$$

5. NUMERICAL SCHEME

Our developed numerical scheme is based on forward Euler time discretization, upwind finite difference approximation of the differential terms, and approximation of the

scattering operator by a matrix operator. The system is abstractly represented by

$$f_t = F(f, \phi), \qquad \Delta\phi = G(f).$$

The second equation is linear and one-dimensional. Its solution is rather trivial. One can solve for ϕ and substitute in the first equation:

$$f_t = F(f, \Delta^{-1}(G(f))).$$

The resulting equation is a non-linear hyperbolic equation. The non-linear term is $\nabla\phi \cdot \nabla_u f$. We denote by f^n the solution at time $n\,\Delta t$. The discretization in time is

$$\frac{f^{n+1} - f^n}{\Delta t} = F(f^n, \phi^n), \qquad \Delta\phi^n = G(f^n).$$

Our discretization in detail is presented below. We define a grid in (z, k, μ, t) space by

$$f^n_{sij} = f(s\,\Delta z, i\,\Delta k, j\,\Delta\mu, n\,\Delta t) = f(z_s, k_i, \mu_j, t_n).$$

Backward difference is defined as $D_z^- f_{sij} = (f_{sij} - f_{s-1,ij})/\Delta z$, with the forward difference as $D_z^+ f_{sij} = (f_{s+1,ij} - f_{sij})/\Delta z$ and the central difference as $D_z^0 f_{sij} = (f_{s+1,ij} - f_{s-1,ij})/2\Delta z$. Using the above notation, our numerical scheme is

$$D_z^+ D_z^- \phi_s^n = \frac{e}{\varepsilon}(n_s - n_{Ds}), \qquad F_s = \frac{e}{m} D_z^0 \phi_s, \tag{8}$$

$$\frac{f^{n+1} - f^n}{\Delta t} + k\mu \frac{\hat f_{s+1/2} - \hat f_{s-1/2}}{\Delta z} + F_z \left\{ \mu \frac{\hat f_{i+1/2} - \hat f_{i-1/2}}{\Delta k} + \frac{2\mu \bar f_i}{k} + \frac{\hat g_{j+1/2} - \hat g_{j-1/2}}{k\,\Delta\mu} \right\} = S_{sij}, \tag{9}$$

$$\bar f_i = \frac{\hat f_{i+1/2} + \hat f_{i-1/2}}{2(1 + \Delta k^2/4k^2)},$$

$$n_s = 2\pi \sum_j \sum_i \left(k_i^2 + \frac{\Delta k^2}{4} \right) f_{sij}\,\Delta k\,\Delta\mu.$$

The definitions for n_s and $\bar f$ are designed such that mass is conserved in each time step. These definitions are motivated by the following argument. Recall that density is calculated via

$$n = 2\pi \iint f(k, \mu)\, k^2\, dk\, d\mu.$$

In the velocity space, mass is conserved since we have $k^2(f_k + 2f/k) = (k^2 f)_k$:

$$\iint F_z \left\{ \mu f_k + \frac{2\mu f}{k} + \frac{((1-\mu^2) f)_\mu}{k} \right\} k^2\, dk\, d\mu = 0.$$

We discretize the terms $f_k + 2f/k$ such that an analogous relation holds for the discretized approximation:

$$\begin{aligned} \Delta k k^2 \left(f_k + \frac{2f}{k} \right) &\approx (k^2 f)_{i+1/2} - (k^2 f)_{i-1/2} \\ &= (k^2_{i+1/2} - k^2_{i-1/2}) f_{i+1/2} + k^2_{i-1/2}(f_{i+1/2} - f_{i-1/2}) \\ &= (k^2_{i+1/2} - k^2_{i-1/2}) f_{i-1/2} + k^2_{i+1/2}(f_{i+1/2} - f_{i-1/2}). \end{aligned}$$

With some manipulation we obtain

$$\begin{aligned} k^2 \left(f_k + \frac{2f}{k} \right) &\approx \frac{1}{2}(k^2_{i+1/2} + k^2_{i-1/2}) \left\{ \frac{f_{i+1/2} - f_{i-1/2}}{\Delta k} + \frac{2(k^2_{i+1/2} - k^2_{i-1/2})}{(k^2_{i+1/2} + k^2_{i-1/2})} \frac{f_{i+1/2} + f_{i-1/2}}{2} \right\} \\ &= \left(k_i^2 + \frac{\Delta k^2}{4} \right) \\ &\quad \times \left\{ \frac{f_{i+1/2} - f_{i-1/2}}{\Delta k} + \frac{2}{k_i} \frac{(f_{i+1/2} + f_{i-1/2})}{2(1 + \Delta k^2/4k_i^2)} \right\}. \end{aligned}$$

Flux functions, $\hat f_{s+1/2}$, $\hat f_{i+1/2}$, and $\hat g_{j+1/2}$ are defined in the following fashion:

$$\begin{aligned} &\hat f_{s+1/2} = f_s && \text{if} \quad k\mu > 0, \\ &\hat f_{s+1/2} = f_{s+1} && \text{if} \quad k\mu < 0, \\ &\hat f_{i+1/2} = f_i && \text{if} \quad F_z\mu > 0, \\ &\hat f_{i+1/2} = f_{i+1} && \text{if} \quad F_z\mu < 0, \\ &\hat g_{j+1/2} = (1-\mu^2) f_j && \text{if} \quad F_z > 0, \\ &\hat g_{j+1/2} = (1-\mu^2) f_{j+1} && \text{if} \quad F_z < 0. \end{aligned}$$

The scattering terms S_{sij} are calculated using trapezoidal rule. The scattering term, s_{ac}, is analytically integrated in the k space. For integrating s_{op}^{em} and s_{op}^{abs} an approximation to the δ function is used. The particular approximation that we used is

$$\delta(x) = \frac{0.75}{\varepsilon} \left(1 - \frac{x^2}{\varepsilon^2} \right) H(1 - x^2).$$

$H(x)$ is the Heaviside function. The scattering operator is reduced to a matrix operator that is computed at the beginning of the calculation and used for the rest of the computation. The trapezoidal rule is used as the integration formula for calculating the moments.

The upwind difference approximation of the first-order terms has the truncation error that contains a second-order

operator with a positive multiplier. The truncation error of our discretization is

$$\frac{\Delta t}{2} f_{tt} - \frac{k\,|\mu|\,\Delta z}{2} f_{zz} - \frac{|F_z \mu|\,\Delta k}{2} f_{kk} - \frac{|F_z \mu|\,\Delta k}{k(1+\Delta k^2/4k^2)} f_k + \frac{|F_z|\,\Delta\mu}{k} f + \frac{2\,|F_z|\,\mu\,\Delta\mu}{k} f_\mu - \frac{|F_z|(1-\mu^2)\,\Delta\mu}{2k} f_{\mu\mu}.$$

The truncation error introduces the so-called artificial viscosity in the method. The second-order operator smooths sharp gradients in the solution. This smoothing effect is reduced by refining the mesh in high gradient regions. An alternative solution is to use high order methods to calculate the fluxes. In the calculations done based on the hydrodynamic model, use of a sixth-order stencil proved to be effective in reducing numerical diffusion in high gradient regions [4]. For BTE calculations, we had to refine the mesh in the areas where the gradient of n_D is high. Our developed scheme for BTE is general and can be extended to higher order methods. Higher order schemes such as ENO schemes can be easily implemented in our code.

Since our time integration is explicit, time steps have to be limited to satisfy the Courant–Friedrichs–Lewy (CFL) condition. Necessary CFL conditions for stability are

$$\frac{k\,|\mu|\,\Delta t}{\Delta z} < 1, \qquad \frac{|F_z \mu|\,\Delta t}{\Delta k} < 1, \qquad \frac{|F_z|\,(1-\mu^2)\,\Delta t}{k\,\Delta\mu} < 1.$$

In practice this translates into

$$\Delta t < \frac{\Delta z}{k_{\max}}, \qquad \Delta t < \frac{\Delta k}{\text{Max}\,|F_z|}, \qquad \Delta t < \frac{k_{\min}\,\Delta\mu}{\text{Max}\,|F_z|}.$$

We used an automatic time stepping based on the above criteria in our calculations and no instability was observed.

6. NUMERICAL RESULTS

For validating the Boltzmann–Poisson code and comparing the two models, we choose the n^+nn^+ structure as is described in Section 4 of this paper. We use similar initial conditions for both computations. The solutions are computed for 5 ps and then compared. In Fig. 3 we show the calculated velocity profile as a function of space. Note that in our scale saturation velocity is 0.1; also note that the spike near $z = 0.7\ \mu$m is missing in the Boltzmann–Poisson solution. We compare the Mach numbers in Fig. 4. Note that the flow is subsonic. The maximum velocity in the solution of BTE is higher than the hydrodynamic model, possibly because the scattering constants are low and/or we need to consider more scattering mechanisms. In Fig. 5 we compare the calculated temperatures from the

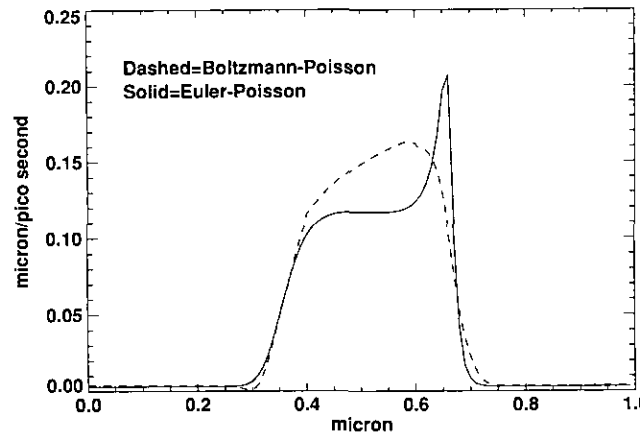

FIG. 3. Electron velocity.

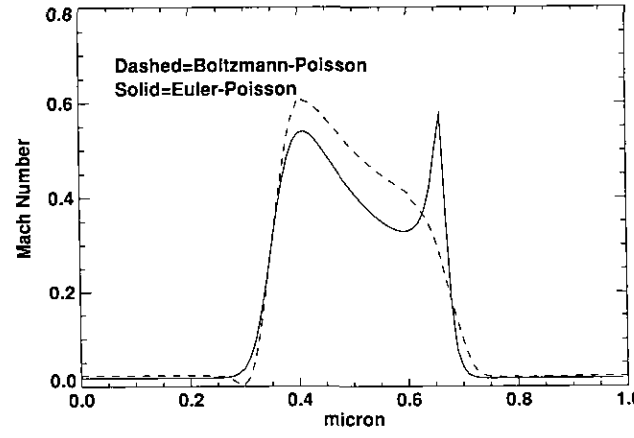

FIG. 4. Mach number of the flow.

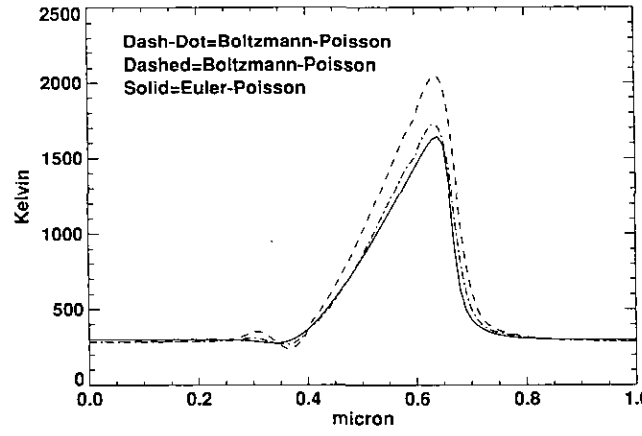

FIG. 5. Temperature (hydro), T_{11}, and T_{33}.

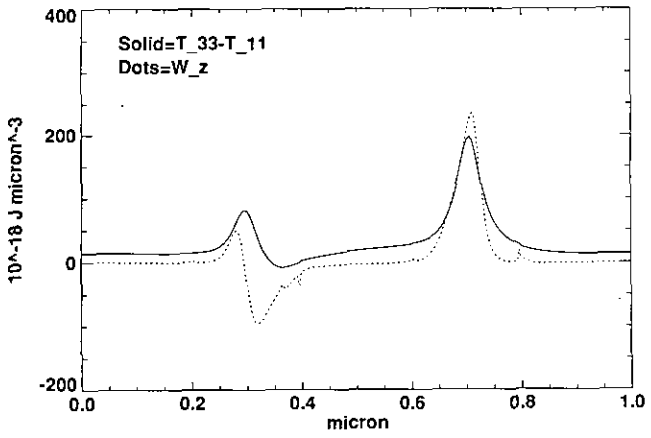

FIG. 6. Viscosity comparison.

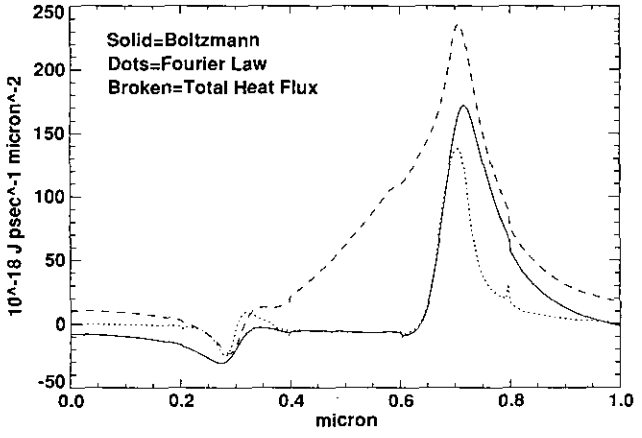

FIG. 7. Heat conduction comparison.

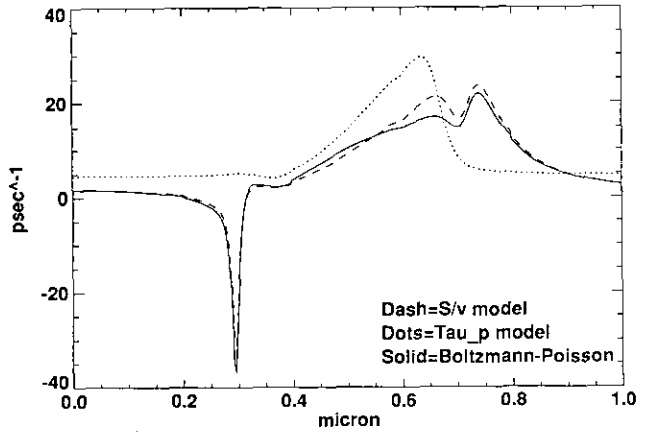

FIG. 8. Momentum relaxation time comparison.

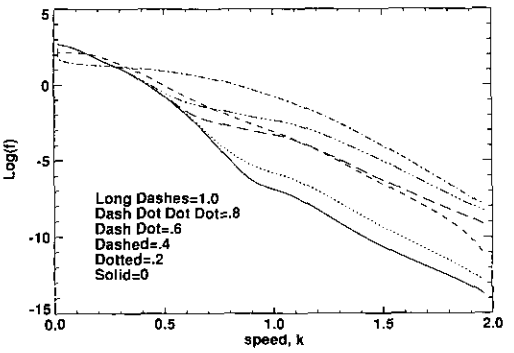

FIG. 9. Density distribution comparison.

hydrodynamic model and the BTE code. We observe that T_{33}, corresponding to the z direction, is a little higher than $T_{11} = (T_{22})$. The difference can be approximated by the viscosity terms. In Fig. 6 we compare the viscosity terms. The solid curve is $n((2T_{33} - T_{22} - T_{11})/3)$ and the dotted line is $-\frac{4}{3}\tau_p nTw_z$. The velocity profile calculated with the viscosity terms included in the hydrodynamic model is very close to the profiles calculated without the viscosity terms (not shown here). The could be expected since the Reynolds number of the flow is around 10^3. In Fig. 7 the solid line shows the heat conduction term from BTE and the doted line shows the heat conduction term calculated from the Fourier law, $\kappa n T_z$, where for κ we use the Wiedmann–Franz law [1]. We observe that the approximation is reasonable except in the drain, where the exact heat conduction term decays slower than the Fourier approximation.

In Fig. 8 we plot τ_p as calculated from the BTE, the model suggested by Baccarani and Wordeman [1], and the model suggested by S. Lee [12]. The unusual dips in the solid line at $z = 0.3$ and $z = 0.7$ are from numerical inaccuracies. The model for τ_p is not accurate. However, two features are observed: First the dependence of τ_p on $1/T$ is too strong. The other feature is that, as electrons enter the drain, the relaxation of the high velocity electrons requires a certain distance. This distance seems to be shorter for relaxation of the second moment (temperature) but longer for both the first moment of the scattering term (momentum relaxation time) and the third moment of the density (heat conduction term). Finally, in Fig. 9, we show the density distribution funcion as a function of k at different locations in the device. The probability density function is integrated over all angles μ and is normalized. The density is close to Maxwellian at $x = 0.0$ and $x = 1.0$ but deviates substantially in the channel.

7. CONCLUSION

We presented a simple scheme for solving the Boltzmann–Poisson system, modeling a one-dimensional electron flow in a semiconductor device. The computer time

is modest for the one-dimensional case. A more efficient algorithm is needed for calculations in two or three space dimensions. The results from the BTE calculations are integrated over velocity space to obtain measurable physical quantities. The results are compared with the results from the hydrodynamic model. The models for heat conduction and viscosity are close, but not accurate. The viscosity term has little effect on the flow and can be neglected. The model for τ_p is very different from our computed τ_p and is one of the factors contributing to the non-physical overshoot. The accuracy of the hydrodynamic model seems to be very bad near the junctions. As the distribution function goes through a radical change, the constitutive relations for closing the Navier–Stokes system fail.

REFERENCES

1. G. Baccarani and M. R. Wordeman, *Solid State Electron.* **28**, 407 (1985).
2. K. Bløtekjær, *IEEE Trans. Electron Devices* **ED-17**, 38 (1970).
3. A. J. Chorin, *Commun. Pure Appl. Math.* **25**, 171 (1972).
4. E. Fatemi, J. Jerome, and S. Osher, *IEEE Trans. Comput. Aided Des. Integr. Circuits Syst.* **10**, No. 2 (1991).
5. E. Fatemi, C. Gardner, J. Jerome, S. Osher, and D. Rose, in *Computational Electronics*, edited by Hess, Leburton, and Ravioli (Kluwer Academic, 1991).
6. G. I. Gamba, *Comm. Partial Differential Equations* **17**, Nos. 3 & 4, 553 (1992).
7. C. L. Gardner, J. W. Jerome, and D. J. Rose, Numerical methods for the hydrodynamic device model: Subsonic flow, *IEEE Trans. Comput. Aided Des. Integr. Circuits Syst.* **8**, 501 (1989).
8. H. L. Grubin and J. P. Kreskovsky, in *VLSI Electronics: Microstructure Science*, Vol. 10, edited by N. G. Einspruch and R. S. Bauer (Academic Press, New York, 1985). p. 237.
9. K. Huang, *Statistical Mechanics* (Wiley, New York, 1987), p. 93.
10. C. Jacoboni and L. Reggiani, *Rev. Mod. Phys.* **55**, No. 3 (1983).
11. H. B. Keller and B. Wendroff, *Commun. Pure Appl. Math.* **10**, 567 (1957).
12. S. Lee, Ph.D. thesis, University of Massachusetts, 1990 (unpublished).
13. B. Niclot, P. Degond, and F. Poupaud, *J. Comput. Phys.* **78**, 313 (1988).
14. F. Odeh, M. Rudan, and J. White, *COMPEL* **5**, 149 (1986).
15. C. W. Shu and S. Osher, *J. Comput. Phys.* **83**, 32 (1989).
16. G. A. Sod, *Commun. Pure Appl. Math.* **30**, 391 (1977).